

# Quantum Many-body Scars through the Lens of Correlation Matrix

Zhiyuan Yao<sup>1,\*</sup> and Pengfei Zhang<sup>2,3,4</sup>

<sup>1</sup>Key Laboratory of Quantum Theory and Applications of MoE,  
Lanzhou Center for Theoretical Physics, and Key Laboratory of Theoretical Physics of Gansu Province,  
Lanzhou University, Lanzhou, Gansu 730000, China

<sup>2</sup>Department of Physics, Fudan University and State Key Laboratory of Surface Physics, Shanghai, 200438, China

<sup>3</sup>Shanghai Qi Zhi Institute, AI Tower, Xuhui District, Shanghai 200232, China

<sup>4</sup>Hefei National Laboratory, Hefei 230088, China

(Dated: October 30, 2024)

Quantum many-body scars (QMBS)—rare eigenstates that evade thermalization—are typically characterized by their low entanglement entropies compared to surrounding thermal eigenstates. However, due to finite-size effects in systems accessible via exact diagonalization, this measure can be ambiguous. To address this limitation, we propose using the correlation matrix spectrum as an alternative probe to identify QMBS. In cases of exact QMBS with either known analytic expressions or can be captured by various frameworks of QMBS, we find the dimensionality of the null space of the correlation matrix—an integer value, and thus immune to finite-size effects—can qualitatively isolate QMBS. Beyond serving as a diagnostic tool, the correlation matrix method enables easy manipulation of the QMBS subspace. For approximate QMBS, such as those in the PXP model, we observe that the correlation matrix spectrum features numerous approximate zero eigenvalues, distinguishing these states. We demonstrate the effectiveness and utility of this method with several paradigmatic QMBS examples.

*Introduction.* With rapid advances in preparing and manipulating quantum states across various artificial quantum platforms, there has been growing interest in understanding how a generic isolated quantum system thermalizes after a quench [1–6]. The universal thermalization imposes stringent constraints on the eigenstates of generic interacting quantum systems, and a widely accepted framework is the eigenstate thermalization hypothesis (ETH), which posits that locally an eigenstate encodes the information of a thermal ensemble [7–11]. Except for systems that are integral [12–14] or with emergent integrability such as the many-body localized systems [5, 15, 16], the validity of ETH has been confirmed in numerous numerical studies [3, 17]. Moreover, it was believed that the ETH applies in the *strong sense* that it holds for every eigenstate with finite energy density [18].

However, the ETH has recently been challenged by persistent oscillations of local observables after a quench in a Rydberg atom chain [19]. Shortly after, it is shown that the ETH in the effective PXP model is valid only in the *weak sense*: it breaks down for a measure-zero subset of eigenstates [20, 21]. These special outliers, drawing analogy to single-particle phenomena [22], were dubbed quantum many-body scars (QMBS), or simply scar states. This discovery sparked intense ongoing research, significantly expanding our understanding of QMBS [23–25]. For example, Shiraishi and Mori have constructed a framework to embed a target space spanned by scar states in a nonintegrable model [26]. Families of Hamiltonians hosting QMBS with closed analytic expressions and equidistant energy separation have also been constructed from symmetry and quasisymmetry perspectives [27–32]. In parallel, in the spirit of  $\eta$ -paring states in the Hubbard model [33, 34], the Mark–Lin–Motrunich (MLM) frame-

work [35] and the equivalent spectrum generating algebra (SGA) formalism [36] have provided unified explanations of scar states discovered across different models [37–43].

However, due to the varying principles underlying those constructions, a unified framework for QMBS is still lacking [24]. As a result, the origin of QMBS in specific models is often addressed on a case-by-case basis. Moreover, theoretical analysis can often become quite involved, making it difficult to identify potential connections between different frameworks. For example, it is unclear whether the second family of QMBS in the spin-1 XY model can be captured by existing formalisms [41, 44]. Additionally, controlling the scar subspace is often challenging. On the numerical side, the entanglement entropy is commonly used to identify QMBS due to their characteristic low-entanglement nature [45]. However, because of the limited system sizes accessible via exact diagonalization, finite-size effects can make it difficult to reliably distinguish QMBS using this approach.

In this Letter, we show that these problems can be well addressed using the correlation matrix spectrum as a tool for characterizing and diagnosing QMBS. For exact QMBS, including those not captured by previous formalisms, we find the dimensionality of the kernel of the correlation matrix—being an integer and immune to finite-size effects—differs from that of thermal eigenstates. This number thus provides a sharp *qualitative* probe of QMBS, superior to the *quantitative* probe of entanglement entropy. For approximate QMBS, such as those in the PXP model, the distinct feature of numerous approximate zero eigenvalues in the correlation matrix spectrum also allow us to single out QMBS from thermal eigenstates.

*Correlation Matrix.* Our work is primarily motivated

by the information perspective of the ETH. According to this hypothesis, the diagonal matrix element of a local observable,  $\hat{O}$ , with respect to a thermal eigenstate  $|n\rangle$  approaches the thermal ensemble average as the system size increases [3, 8, 9]

$$\langle n|\hat{O}|n\rangle \rightarrow \frac{1}{Z} \text{Tr} e^{-\beta\hat{H}} \hat{O}, \quad (1)$$

where  $Z = \text{Tr} e^{-\beta\hat{H}}$  is the partition function and  $\beta$  represents the inverse temperature (with  $k_B = 1$ ). This implies that a thermal eigenstate encodes sufficient information to infer the underlying Hamiltonian, consistent with the fact that a wavefunction has exponentially many components, while a local Hamiltonian has only extensively many parameters. In other words, one might not be able to reconstruct the Hamiltonian from a low-entangled QMBS. These ideas are solidified by using the correlation matrix, originally introduced in [46], as an operational tool for reconstructing the underlying local Hamiltonian from a single eigenstate. Let  $|\psi\rangle$  be a wave function, and let  $\mathcal{V}$  denote a real vector space of Hermitian operators spanned by a set of operator basis  $\{\hat{L}_i\}$  that acts on  $|\psi\rangle$ . For an arbitrary Hermitian operator  $\hat{O} = \sum_i w_i \hat{L}_i \in \mathcal{V}$ , we have the following inequality

$$\langle \psi|\hat{O}^2|\psi\rangle - (\langle \psi|\hat{O}|\psi\rangle)^2 = \langle \psi_\perp|\psi_\perp\rangle \geq 0, \quad (2)$$

where  $\hat{O}|\psi\rangle = \xi|\psi\rangle + |\psi_\perp\rangle$ , and  $|\psi_\perp\rangle$  is orthogonal to  $|\psi\rangle$ , i.e.,  $\langle \psi|\psi_\perp\rangle = 0$ . This inequality can be casted into a quadratic form

$$\mathbf{w}^T \cdot \mathbf{M} \cdot \mathbf{w} \geq 0, \quad (3)$$

where  $\mathbf{w} \equiv (w_1, w_2, \dots)^T$  is a vector of coefficients, and  $\mathbf{M}$  is the real symmetric *correlation matrix* defined as

$$M_{ij} = \frac{1}{2} \langle \psi|(\hat{L}_i \hat{L}_j + \hat{L}_j \hat{L}_i)|\psi\rangle - \langle \psi|\hat{L}_i|\psi\rangle \langle \psi|\hat{L}_j|\psi\rangle. \quad (4)$$

The correlation matrix  $\mathbf{M}$  is positive semidefinite, and equality in the quadratic form is attained only when  $\mathbf{w}$  belongs to its null space,  $\mathbf{w} \in \text{Ker}(\mathbf{M})$ . In this case, the corresponding  $\hat{O}$  is referred to as an *eigenoperator* of  $|\psi\rangle$ , meaning  $\hat{O}|\psi\rangle = \xi|\psi\rangle$ . Let  $N_0 \equiv \dim(\text{Ker}(\mathbf{M}))$  denote the dimensionality of the null space of  $\mathbf{M}$ . We can then construct  $N_0$  linear-independent eigenoperators of  $|\psi\rangle$ . If the original Hamiltonian belongs to the chosen operator space  $\mathcal{V}$ , then the uniqueness of Hamiltonian reconstruction from thermal eigenstates is equivalent to  $N_0 = 1$  [46]. We shall see below exact QMBS are characterized by a often much larger  $N_0$ .

*Exact QMBS.* A paradigmatic model that hosts exact QMBS is the one-dimensional Affleck–Kennedy–Lieb–Tasaki (AKLT) Hamiltonian

$$\hat{H}_0 = \sum_i \left[ \frac{1}{2} \hat{\mathbf{S}}_i \cdot \hat{\mathbf{S}}_{i+1} + \frac{1}{6} (\hat{\mathbf{S}}_i \cdot \hat{\mathbf{S}}_{i+1})^2 + \frac{\hat{\mathbb{I}}}{3} \right], \quad (5)$$

where  $\hat{\mathbf{S}}_i$  is the spin-1 operator at site  $i$ , and  $\hat{\mathbb{I}}$  is the identity operator [37, 38, 47]. The known series of QMBS  $|\mathcal{S}_{2n}\rangle$  have eigenenergies of  $E_n = 2n$  and are captured by the SGA formalism. Their explicit form is given by

$$|\mathcal{S}_{2n}\rangle = (\hat{Q}^+)^n |G\rangle, \quad n = 0, 1, \dots, \quad (6)$$

where  $|G\rangle$  is the ground state of the AKLT model and  $\hat{Q}^+ = \sum_{i=1}^L (-1)^i (\hat{S}_i^+)^2$  with  $\hat{S}_i^+$  being the spin-1 raising operator at site  $i$  [35, 36]. Interestingly, this scar tower  $\{|\mathcal{S}_{2n}\rangle\}$  is stable against certain disorder perturbations: they persist as eigenstates of the following disordered Hamiltonian  $\hat{H} = \hat{H}_0 + \hat{H}_{\text{dis}}$ ,

$$\hat{H} = \hat{H}_0 + \sum_{n,m,m'} [\xi_{m,m'}^n (|J_{2,m}\rangle \langle J_{2,m'}|)_{n,n+1} + \text{h.c.}], \quad (7)$$

where  $n$  indexes lattice sites,  $m$  and  $m'$  are restricted to take  $-2, -1, 0$  in the summation,  $\xi_{m,m'}^n$  are arbitrary complex numbers, and  $|J_{j,m}\rangle$  inside the parenthesis is the total spin  $j$ , total magnetization  $m$  state of two spins at sites  $n$  and  $n+1$  [35].

To show that the number of correlation matrix zeros  $N_0$  can distinguish scar states from thermal eigenstates, we start with simple range-2 local basis  $\hat{L}_i$ . Just like Pauli matrices for spin-1/2 systems, we can use the standard generators of the SU(3) group, the eight Gell-Mann matrices  $\lambda_a (a = 1, 2, \dots, 8)$ , together with the identity matrix  $\lambda_0$  to define the operator bases  $\hat{L}_i$ ,

$$\hat{L}_i = (\lambda_a \otimes \lambda_b)_{n,n+1}, \quad (8)$$

where  $n = 1, 2, \dots, L$  labels the lattice sites ( $L+1$  is identified as 1) and  $\hat{L}_i$  acts nontrivially only on sites  $n$  and  $n+1$ . Here  $a = 0, 1, \dots, 8$  and  $b = 1, 2, \dots, 8$  so that we include all single-site and two-site operators but exclude the trivial identity operator, which makes the correlation matrix  $M$  of dimension  $72L \times 72L$ . Since we can linearly combine  $\hat{L}_i$  to construct the Hamiltonian (7), we have  $N_0 \geq 1$  for every eigenstate. As illustrated in Fig. 1, eigenstates with energies  $E_n = 0, 2, \dots, L$  indeed exist and are numerically checked to correspond to SGA scar states  $|\mathcal{S}_{2n}\rangle$ . Additionally, other scar states with anomalously low bipartite entanglement entropies are observed. On the side of correlation matrix spectrum, all thermal eigenstates unanimously have  $N_0 = 1$ , meaning the original Hamiltonian can be reconstructed from a single thermal eigenstate [46]. In contrast, all the scar states exhibit larger values of  $N_0$ , making the correlation matrix zeros a reliable *qualitative* probe for scar states. This stands in contrast to the *quantitative* probe of entanglement entropy, which is prone to finite-size effects.

Furthermore, analytical results otherwise difficult to derive can be obtained. Further analysis shows that, at least for  $L = 6, 8, \dots, 16$ , the minimal number of  $N_0$  of SGA scar states satisfies  $N_0^{(\text{min})} = 9L + 3$ . This number

has to be compared with the known  $9L + 2$  Hermitian eigenoperators of the SGA scar state: the Hamiltonian  $\hat{H}_0$ ; the total magnetization  $\hat{S}^z = \sum_i \hat{S}_i^z$ ;  $9L$  Hermitian disorder terms in  $\hat{H}_{\text{dis}}$ . This means there is an additional linearly independent range-2 operator, denoted as  $\hat{A}$ , that is the eigenoperator of all SGA scar states. Thus, the most general range-2 Hamiltonian hosting the SGA scar states is  $\hat{H} + \xi \hat{A}$  where  $\xi$  is an arbitrary real number. The explicit form of  $\hat{A}$  is given by

$$\hat{A} = \sum_n (-1)^n \hat{A}_n, \quad (9)$$

where  $\hat{A}_n$  in matrix representation reads

$$\begin{aligned} \hat{A}_n = & \sum_{a=1}^8 c_a (\lambda_a \otimes \lambda_a)_{n,n+1} + 2(\lambda_1 \otimes \lambda_6 + 1 \leftrightarrow 6)_{n,n+1} \\ & + 2(\lambda_2 \otimes \lambda_7 + 2 \leftrightarrow 7)_{n,n+1} \\ & + \frac{4}{\sqrt{3}} (\lambda_3 \otimes \lambda_8 + 3 \leftrightarrow 8)_{n,n+1}. \end{aligned} \quad (10)$$

with  $c_n = (-11/3, -11/3, -5, 1, 1, 53/3, 53/3, 7)$  accurate to machine precision. We have also tested that for even system sizes ranging from  $L = 6$  to  $L = 16$ , the constructed operator  $\hat{A}$  annihilates all the SGA scars in the AKLT model. Although the prime numbers appearing in  $c_n$  suggest the difficulty of deriving this result analytically, it can be easily obtained by analyzing the null space of the correlation matrix numerically. For the additional scar states, we have successfully obtained their analytical expressions as well [48]. In short, these states are highly excited states of the AKLT Hamiltonian  $\hat{H}_0$  that are preserved under inclusion of the disorder term  $\hat{H}_{\text{dis}}$ .

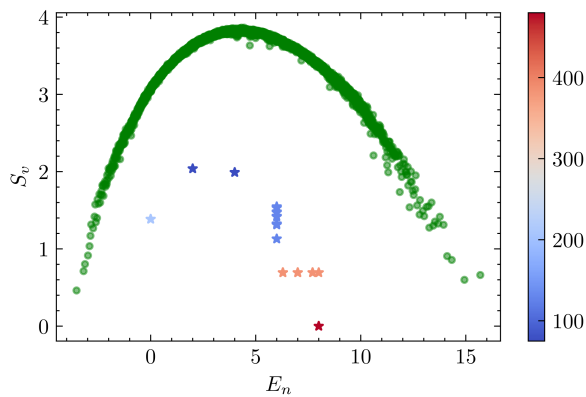


FIG. 1. Plot showing the bipartite entanglement entropies of the eigenstates of the disordered AKLT Hamiltonian (7) against their eigenenergies. Thermal eigenstates are represented by green circles, all uniformly having  $N_0 = 1$ . Scar states are highlighted with stars, and their corresponding  $N_0$  values are color-coded according to the color bar.

*Scar Embedding and Compatibility.* In addition to providing a qualitative diagnosis of scar states, the corre-

lation matrix framework enables flexible manipulation of the scar state subspace and offers insight into its internal structure. Let  $\mathcal{A}_{|\psi\rangle}$  denote the *eigenoperator space* of  $|\psi\rangle$ , which is the operator space spanned by  $\{\hat{A} = \sum_i w_i \hat{L}_i\}$ , where  $\mathbf{w}$  is the null eigenvector of the correlation matrix  $\mathbf{M}$  constructed from  $|\psi\rangle$ . Given two eigenstates  $|\psi\rangle$  and  $|\phi\rangle$  of a Hamiltonian  $\hat{H}$ , if  $\mathcal{A}_{|\psi\rangle} \subset \mathcal{A}_{|\phi\rangle}$ , then we can always select an operator  $\hat{A} \notin \mathcal{A}_{|\phi\rangle}$  from  $\mathcal{A}_{|\psi\rangle}$  and add it to the original Hamiltonian to construct a new Hamiltonian,

$$\hat{H}' = \hat{H} + \hat{A}, \quad (11)$$

of which  $|\phi\rangle$  but not  $|\psi\rangle$  remains an eigenstate. To illustrate this, we use the disordered AKLT model (7) as an example. Scar states in this model include the ferromagnetic state  $|F\rangle = |11 \cdots 11\rangle$  where  $m_i \equiv 1$ , the single-magnon state,

$$|1_k\rangle = \sum_n e^{ikn} |\underbrace{1 \cdots 1}_{n-1} 0 \underbrace{1 \cdots 1}_{L-n}\rangle, \quad (12)$$

where  $n = 0, 1, \dots, L-1$  in the summation and  $k = 2\pi m/L$  ( $m = 0, 1, \dots, L-1$ ) is the quasimomentum, and several other families such as the SGA tower [49]. A detailed analysis of the eigenoperator spaces reveals that,

$$\mathcal{A}_{|1_k\rangle} \subset \mathcal{A}_{|F\rangle}, \quad \forall k \quad (13)$$

and that  $\mathcal{A}_{|1_k\rangle}$  is not a subset of the eigenoperator space of any other scar. Moreover, although the dimension of  $\mathcal{A}_{|1_k\rangle}$  is the same for all  $k$ , their individual eigenoperator spaces are different. This means that we can construct a Hamiltonian to retain any given  $|1_k\rangle$  and  $|F\rangle$  as the only scar states. We can also add terms to make  $|F\rangle$  the unique scar state. However, for Hamiltonian with on-site and nearest-neighbor interactions, if  $|1_k\rangle$  is a scar state,  $|F\rangle$  is necessarily an eigenstate. As shown in Fig. 2, we can construct a Hamiltonian  $\hat{H}' = \hat{H} + \sum_i \xi_i \hat{A}_i$  where  $\hat{A}_i \in \mathcal{A}_{|1_\pi\rangle}$  and  $\xi_i$  are random numbers to embed scar space  $\mathcal{S} = \text{span}\{|1_\pi\rangle, |F\rangle\}$  spanned by  $|1_\pi\rangle$  and  $|F\rangle$ . Similarly, since the eigenoperator space  $\mathcal{A}_{|G\rangle}$  is not a subset of any other scar, we can construct a Hamiltonian with  $|G\rangle$  as the only scar state [50].

*Unification and Generality.* Our method of using correlation matrix zeros  $N_0$  to probe exact QMBS unifies many mathematical frameworks. To illustrate the generality of our approach, we consider three prominent examples: the Shiraishi–Mori framework, the non-Abelian Lie algebra construction, and the SGA formalism. In the Shiraishi–Mori formalism [26], the scarring Hamiltonian takes the following form

$$\hat{H} = \sum_i \hat{P}_i \hat{h}_i \hat{P}_i + \hat{H}', \quad (14)$$

where  $\hat{P}_i$  are a set of local projectors that annihilate the scar subspace  $\mathcal{S}$ ,  $\hat{h}_i$  are some local Hermitian operators,

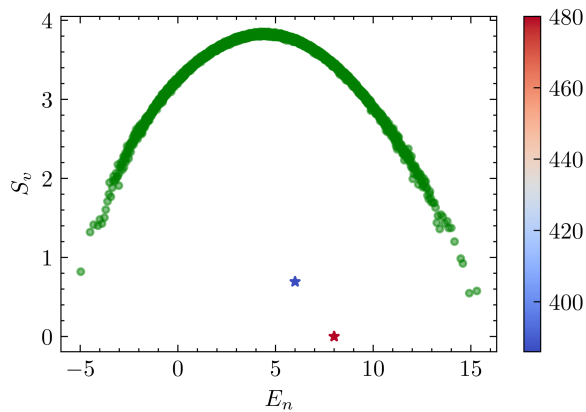


FIG. 2. Plot of bipartite entanglement entropies against eigenenergies of a Hamiltonian  $\hat{H}'$  that embeds the  $|1_{k=\pi}\rangle$  and  $|F\rangle$  states as the only scar states. The scar states are represented by stars, with their colors corresponding to the values of  $N_0$  as indicated by the color bar.

and  $\hat{H}'$  is some Hamiltonian that satisfies  $[\hat{P}_i, \hat{H}']\mathcal{S} = 0$ . It follows that for any scar state  $|\psi\rangle \in \mathcal{S}$ , the projector  $\hat{P}_i$  is an eigenoperator of  $|\psi\rangle$  and each  $\hat{P}_i$  contributes a zero eigenvector to the correlation matrix  $\mathbf{M}$  for appropriate large operator space  $\mathcal{V}$ . This means that for any scar state  $N_0 \geq N_p$  where  $N_p$  is the number of projectors  $\hat{P}_i$ , which distinguish it from thermal eigenstates. Similarly, in the “tunnels to towers” construction [32], the scarring Hamiltonian take the following form

$$\hat{H} = \hat{H}_{\text{sym}} + \hat{H}_{\text{SG}} + \hat{H}_A, \quad (15)$$

where  $\hat{H}_{\text{sys}}$  is a Hamiltonian with non-Abelian symmetry to endow the spectrum with a degenerate subspace,  $\hat{H}_{\text{SG}}$  consists of a linear combination of generators in the Cartan subalgebra to lift the degeneracy, and a final Hamiltonian  $\hat{H}_A$  that annihilates a targeted subspace  $\mathcal{S}$  is needed to break symmetries and promote  $\mathcal{S}$  to a scar subspace. In this case,  $\hat{H}_A$  is also an eigenoperator for the scar states, making it detectable via the correlation matrix approach.

To demonstrate that our method also captures QMBS in the SGA formalism [36], it is convenient to use the equivalent Mark–Lin–Motrunich (MLM) framework [35]

$$\left([\hat{H}, \hat{Q}^+] - \epsilon \hat{Q}^+\right) \mathcal{S} = 0, \quad (16)$$

where  $\mathcal{S}$  is the scar subspace,  $\hat{H}$  is the Hamiltonian, and  $\hat{Q}^+$  is the ladder operator that repeatedly acts on a reference eigenstate  $|\psi_0\rangle$  to generates the whole scar tower  $\{|\psi_n\rangle \equiv (\hat{Q}^+)^n |\psi_0\rangle\}$ . Therefore, as long as  $\hat{H}$  and  $\hat{Q}^+$  are sum of local operators with maximum range  $k$ , the left hand, denoted as  $\hat{A}$ , of (16) is of sum of local operators. Although  $\hat{A}$  is in general not Hermitian, this can be easily remedied by choose the operator basis  $\{\hat{L}_i\}$  to be non-Hermitian and subsequently modify the form of

correlation matrix  $M$  as

$$M_{ij} = \langle \psi | \hat{L}_i^\dagger \hat{L}_j | \psi \rangle - \langle \psi | \hat{L}_i^\dagger | \psi \rangle \langle \psi | \hat{L}_j | \psi \rangle. \quad (17)$$

The correlation matrix  $M$  is then a positive semidefinite Hermitian matrix and annihilator  $\hat{A}$  is also one-to-one correspondence with the null eigenvector of  $\mathbf{M}$ . In fact, as demonstrated in the disordered AKLT model, even using a Hermitian operator basis with a real symmetric  $\mathbf{M}$  is often sufficient in detecting scar states.

*Approximate QMBS.* For several paradigmatic exact QMBS we have tested [51], all scar states distinguish themselves from thermal eigenstates by having a much larger  $N_0$ . However, for approximate scars with neither known analytic expressions nor can be captured by previous mathematical formalisms, the single number  $N_0$  may be inadequate. A prime example of this is the well-known PXP model, described by the following Hamiltonian [20, 21]

$$\hat{H} = \sum_i \hat{P}_{i-1} \hat{X}_i \hat{P}_{i+1}, \quad (18)$$

where  $\hat{P}_i = (1 - \hat{Z}_i)/2$  is the projection operator at site  $i$ , and  $\hat{X}_i$  and  $\hat{Z}_i$  are standard Pauli operators. Except for special eigenstates in the middle of the spectrum, the analytic expressions of QMBS are, in general, unavailable [52]. In our correlation matrix study, we choose the matrix representation of range- $k$  operator basis  $\hat{L}_i$  acting on lattice sites  $n+1, n+2, \dots, n+k$  as

$$\hat{L}_i = (\sigma_{a_1} \otimes \sigma_{a_2} \cdots \otimes \sigma_{a_k})_n, \quad (19)$$

where  $\sigma_{a_j}$  denotes identity and three Pauli matrices ( $X, Y, Z$ ) for  $a_j = 0$  and  $a_j = 1, 2, 3$ , respectively. As before,  $a_1$  is restricted to 1, 2, 3 while other  $a_i$  take 0, 1, 2, 3. This ensures that our operator basis excludes trivial identity operators but includes all nontrivial local operators up to range  $k$ . We employ periodic boundary conditions in our study. As shown in Fig. 3(b), the scar state (colored black) has the same  $N_0$  as those of thermal eigenstates, which is associated with the Rydberg blockade condition. However, the correlation matrix spectrum reveals marked differences between the scar states and the thermal states. To quantify these differences, we introduce the following measure analogous to the role of entanglement entropy in quantifying quantum entanglement

$$n_c = \langle e^{-\lambda_i} \rangle \equiv \frac{1}{N} \sum_{i=1}^N e^{-\lambda_i}, \quad (20)$$

to characterize the correlation matrix spectrum, where the summation over  $\lambda_i$  is restricted to nonzero values and  $N$  is the total number of nonzero  $\lambda_i$ . As can be seen from Fig. 3(c), the introduced quantity  $n_c$  effectively distinguishes scar states from thermal eigenstates. Moreover,  $n_c$  is less sensitive to finite-size effects compared to entanglement entropy, making it a more reliable probe.

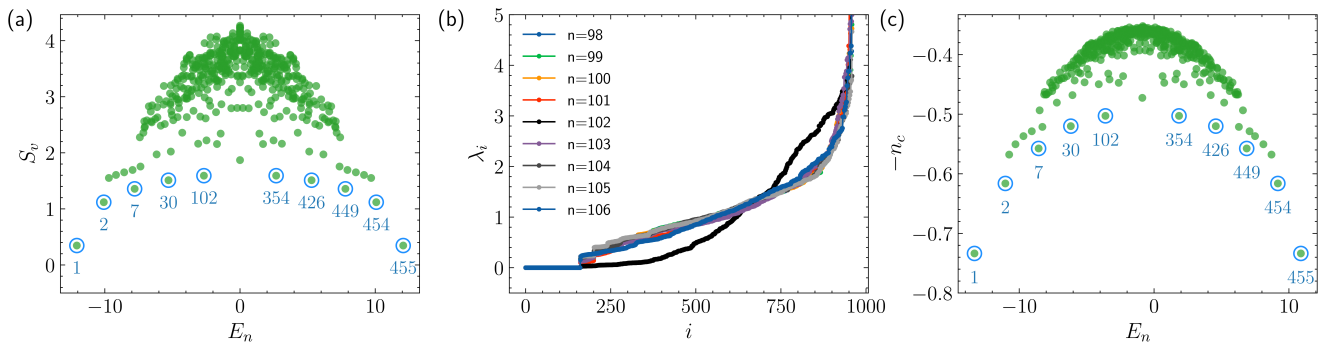


FIG. 3. (a) Bipartite von Neumann entanglement entropy  $S_v$  of eigenstates plotted against the eigenenergies of the PXP model for  $L = 20$  in the  $(k, I) = (0, 1)$  sector, where  $k$  is the lattice momentum and  $I$  is the parity quantum number. The QMBS are marked with blue circles with annotated numbers below designating the eigenstate index  $n$  as eigenenergy increases. (b) Correlation matrix spectra for the scar state  $n = 102$  (black dots) and the surrounding thermal eigenstates (colored dots). (c) Plot of  $-n_c$  against the eigenenergies of the PXP model for  $L = 20$  and  $(k, I) = (0, 1)$ . The blue circles and annotated text have the same meaning as in panel (a).

*Summary.* We have introduced a new method to detect quantum many-body scars (QMBS) using the correlation matrix spectrum. For exact QMBS, we demonstrate that the integer  $N_0$ , the number of zero eigenvalues, can *qualitatively* distinguish scar states from thermal eigenstates. In this regard,  $N_0$  functions similarly to how symmetry and topological numbers are used to classify phases of matter. Our method not only unifies many previous frameworks of QMBS, similar to the recent commutant algebra formalism [53] which we learned after the main idea is developed, but also is quite accessible and flexible. It enables the straightforward derivation of otherwise obscure analytic results, manipulation of the scar subspace, and insights into its internal constraints. For approximate QMBS where  $N_0$  may fall short, one can introduce quantities such as  $n_c$  to characterize scar states, leveraging the presence of multiple approximate zero eigenvalues in the spectrum. Given the versatility of the correlation matrix approach, we anticipate that its applications will extend beyond the study of QMBS.

*Acknowledgments.* We thank Hui Zhai, Lei Pan, and Shang Liu for numerous useful discussions. We also thank Shang Liu for carefully reading our manuscript and valuable feedback. We acknowledge support by NSFC Grant No. 12304288 (Z. Y.), No. 12247101 (Z. Y.), and No. 12374477 (P. Z.).

### Appendix A: The Nature of Additional QMBS in the Disordered AKLT Model

As discussed in the main text, we discovered additional QMBS in the disordered AKLT model,  $\hat{H} = \hat{H}_0 + \hat{H}_{\text{dis}}$ , beyond the known SGA scar states. For convenience, we

shall reproduce the Hamiltonian here,

$$\hat{H} = \hat{H}_0 + \sum_n \sum_{m, m'} [\xi_{m, m'}^n (|J_{2, m}\rangle \langle J_{2, m'}|)_{n, n+1} + h.c.] \quad (21)$$

where  $\hat{H}_0$  is the standard AKLT Hamiltonian, the summation over  $m$  and  $m'$  is restricted to  $m, m' = -2, -1, 0$ , and  $\xi_{m, m'}^n$  are arbitrary complex numbers. Given that a series of low-entanglement eigenstates beyond the ground state have been recently identified [37], we hypothesize that some of these states remain eigenstates with the addition of the disordered term  $\hat{H}_{\text{dis}}$ . In the following, we demonstrate that this is indeed the case. To facilitate this analysis, we first introduce the Schwinger boson representation. Since we are dealing with  $S = 1$  spins, the Schwinger boson creation (annihilation) operators  $\hat{a}_i^\dagger$  ( $\hat{a}_i$ ) and  $\hat{b}_i^\dagger$  ( $\hat{b}_i$ ) at site  $i$  satisfy the following constraint,

$$\hat{a}_i^\dagger \hat{a}_i + \hat{b}_i^\dagger \hat{b}_i = 2, \quad \forall i. \quad (22)$$

The local basis  $|m\rangle_i$  ( $m = -1, 0, 1$ ) are then obtained by acting on the vacuum state of no bosons  $|0\rangle$  with Schwinger boson creation operators

$$|1\rangle_i = \frac{(a_i^\dagger)^2}{\sqrt{2}} |0\rangle, \quad |0\rangle_i = a_i^\dagger b_i^\dagger |0\rangle, \quad |-1\rangle_i = \frac{(b_i^\dagger)^2}{\sqrt{2}} |0\rangle. \quad (23)$$

For assist theoretical analysis, we introduce some graphical notations: a labeled circle represents a local site, an up arrow for  $a^\dagger$ , a down arrow for  $b^\dagger$ , and a right line with middle arrow connecting sites  $n$  and  $n+1$ ,  $\circ \rightarrow \circ$ , for the singlet operator  $\hat{c}_{n, n+1} \equiv \hat{a}_n^\dagger \hat{b}_{n+1}^\dagger - \hat{b}_n^\dagger \hat{a}_{n+1}^\dagger$ . The state is then obtained by acting the operators on the boson vacuum state  $|0\rangle$ . For example, according to (23), the state represented by the following figure

$$|\psi\rangle = \begin{array}{c} \begin{array}{ccc} \circ \uparrow & \rightarrow & \circ \uparrow \\ n & & n+1 \end{array} \\ = \hat{a}_n^\dagger (\hat{a}_n^\dagger \hat{b}_{n+1}^\dagger - \hat{b}_n^\dagger \hat{a}_{n+1}^\dagger) \hat{a}_{n+1}^\dagger |0\rangle \end{array}$$

in the spin basis reads

$$|\psi\rangle = \sqrt{2} \left( |10\rangle_{n,n+1} - |01\rangle_{n,n+1} \right). \quad (24)$$

And the ground state  $|G\rangle$  of the standard AKLT Hamiltonian  $\hat{H}_0$  can be represented as

$$|G\rangle = \dots \rightarrow \textcircled{\circ\circ} \rightarrow \textcircled{\circ\circ} \rightarrow \textcircled{\circ\circ} \rightarrow \textcircled{\circ\circ} \rightarrow \dots \quad (25)$$

With these notations in place, we now proceed to demonstrate that certain low-entangled eigenstates are annihilated by the disordered term  $\hat{H}_{\text{dis}}$ , meaning they remain eigenstates of the disordered AKLT Hamiltonian.

### The ferromagnetic state

The fully polarized ferromagnetic state  $|F\rangle = |11 \dots 11\rangle$  is an eigenstate of the Hamiltonian  $\hat{H}$  with eigenenergy  $E = L$ , as  $\hat{H}_0 |F\rangle = L |F\rangle$ , and  $|F\rangle$  is annihilated by the disordered term. The action of  $(\hat{S}_n^+)^2$  on the ground state  $|G\rangle$  can be illustrated as

$$|M_n\rangle = \dots \rightarrow \textcircled{\uparrow\uparrow} \textcircled{\uparrow\uparrow} \textcircled{\uparrow\uparrow} \rightarrow \dots \quad (26)$$

$n-1 \quad n \quad n+1$

and thus  $(S_n^+)^2 (S_{n+1}^+)^2 |G\rangle = 0$ . The highest SGA scar state,  $|\mathcal{S}_L\rangle$ , corresponds to  $|F\rangle$  when  $L/2$  is even, but does not exist when  $L/2$  is odd. Therefore, as long as  $L$  is even, we have a series of scar states with energies  $E = 0, 2, \dots, L$ , and we shall ascribe  $|F\rangle$  as part of SGA scar family for convenience.

### Single-magnon state $|1_k\rangle$

The single-magnon state  $|1_k\rangle$  defined below (normalization which are unimportant are omitted from below)

$$|1_k\rangle \equiv \sum_n e^{ikn} |n\rangle \quad (27)$$

where  $k = 2\pi m/L$  with  $m = 0, 1, \dots, L-1$  is the lattice momentum, and  $|n\rangle$  in the spin basis reads

$$|n\rangle = \left| \underbrace{1 \dots 1}_{n-1} \underbrace{0 1 \dots 1}_{L-n} \right\rangle. \quad (28)$$

This state is known to be the eigenstate of the AKLT Hamiltonian  $\hat{H}_0$ . Since  $\hat{H}_0$  is a sum of projectors  $\hat{H}_0 = \sum_n \hat{P}_{n,n+1}^{(2)}$ , where  $\hat{P}_{n,n+1}^{(2)}$  projects onto the total spin  $J = 2$  state between neighboring sites, it follows that,

$$\hat{H}_0 |n\rangle = (L-1) |n\rangle + \frac{1}{2} (|n-1\rangle + |n+1\rangle) \quad (29)$$

where we have used  $\hat{P}^{(2)} |11\rangle = |11\rangle$  and  $\hat{P}^{(2)} |01\rangle = \hat{P}^{(2)} |10\rangle = \frac{1}{2} (|10\rangle + |01\rangle)$ , with subscripts  $n, n+1$  suppressed for clarity. Equation (29) describes a single-particle hopping model, making  $|1_k\rangle$  an eigenstates of  $\hat{H}_0$ . Furthermore, since the total  $J_z$  any neighboring spins is either one or two,  $|n\rangle$  is annihilated by disorder terms,  $|J_{2,m}\rangle \langle J_{2,m'}|$  for  $m, m' = -2, -1, 0$ . Therefore,  $|1_k\rangle$  also remains an eigenstate of the disordered AKLT Hamiltonian  $\hat{H}$ . The eigenenergy of  $|1_k\rangle$  is  $E_k = (L-1) + \cos k$ . Alongside the SGA scars, which have eigenenergies  $E = 0, 2, \dots, L$ , these states account for all scar states except for the degenerate ones at  $E = L-2$ .

### $|2_n\rangle$ state

The  $|2_n\rangle$  state with  $n = 0, 1, 3, 4, \dots$

$$|2_n\rangle = \sum_{m=1}^L (-1)^m |m, m+n\rangle, \quad (30)$$

is another family of low-entangled eigenstates of the AKLT Hamiltonian  $\hat{H}_0$ . The maximum  $n$  is  $L/2$  for even  $L/2$  and  $L/2 - 1$  for odd  $L/2$ . Here the two-dimer basis  $|m, m+n\rangle$  graphically reads (configurations at irrelevant sites suppressed)

$$|m, m\rangle = \textcircled{\uparrow\uparrow} \textcircled{\circ\circ} \textcircled{\circ\circ} \textcircled{\uparrow\uparrow}, \quad (31)$$

$m-1 \quad m \quad m+1 \quad m+2$

$$|m, m+1\rangle = \textcircled{\uparrow\uparrow} \textcircled{\uparrow\uparrow} \textcircled{\circ\circ} \textcircled{\circ\circ} \textcircled{\uparrow\uparrow} \textcircled{\uparrow\uparrow}, \quad (32)$$

$m \quad m+1 \quad m+2$

for  $n = 0$  and  $n = 1$ , and for  $n \geq 3$

$$\textcircled{\uparrow\uparrow} \textcircled{\uparrow\uparrow} \textcircled{\uparrow\uparrow} \textcircled{\circ\circ} \textcircled{\circ\circ} \textcircled{\uparrow\uparrow} \textcircled{\uparrow\uparrow} \textcircled{\uparrow\uparrow} \textcircled{\uparrow\uparrow} \textcircled{\uparrow\uparrow} \textcircled{\uparrow\uparrow}. \quad (33)$$

$m \quad m+1 \quad m+n$

From this Schwinger boson representation, it is evident that  $|2_n\rangle$  with  $n \geq 3$  remains the eigenstate of  $\hat{H}$ . This is because the minimum  $J_z$  for any pair of neighboring sites is one, and therefore  $|2_n\rangle$  is annihilated by the disorder term  $\hat{H}_{\text{dis}}$ . The building block of  $|2_{n=1}\rangle = \sum_m (-1)^m |m, m+1\rangle$  is given by

$$\frac{1}{\sqrt{2}} |m, m+1\rangle = \frac{1}{\sqrt{2}} \textcircled{\uparrow\uparrow} \textcircled{\uparrow\uparrow} \textcircled{\circ\circ} \textcircled{\circ\circ} \textcircled{\uparrow\uparrow} \textcircled{\uparrow\uparrow}$$

$m \quad m+1 \quad m+2$

$$= |11001\rangle - 2 |1, 1, -1, 1, 1\rangle - |10101\rangle + |10011\rangle, \quad (34)$$

where irrelevant site configurations have been omitted for clarity, and the first and the last term cancel upon  $(-1)^m$  summation. In the local spin basis representation, when considering the action of  $\hat{H}_{\text{dis}}$  on  $|m, m+1\rangle$ , only the

bonds  $(m, m+1)$  and  $(m+1, m+2)$  are relevant. For the bond  $(m, m+1)$ , we have

$$|00\rangle - 2|1, -1\rangle = -\sqrt{3}|J_{0,0}\rangle - \sqrt{2}|J_{1,0}\rangle, \quad (35)$$

and for the bond  $(m+1, m+2)$ , we have

$$|00\rangle - 2|-1, 1\rangle = -\sqrt{3}|J_{0,0}\rangle + \sqrt{2}|J_{1,0}\rangle. \quad (36)$$

Neither of these bonds contains components of  $|J_{2,m'}\rangle$ ,  $m' = -2, -1, 0$ . Hence  $|2_{n=1}\rangle$  is annihilated by the disorder term  $\hat{H}_{\text{dis}}$ , and  $|2_{n=1}\rangle$  remains an eigenstate of  $\hat{H}$ . However, the  $|n, n\rangle$  state in local spin basis reads

$$\begin{aligned} |m, m\rangle &= \begin{array}{cccc} \uparrow\uparrow & \circ\circ & \circ\circ & \uparrow\uparrow \\ m-1 & m & m+1 & m+2 \end{array} \\ &= 2(|1, 1, -1, 1\rangle + |1, -1, 1, 1\rangle - |1001\rangle) \end{aligned} \quad (37)$$

and  $|00\rangle$  in  $|1001\rangle$  can not be annihilated by  $|J_{2,m'}\rangle\langle J_{2,m'=0}|$ , meaning  $|2_{n=0}\rangle$  ceases to be an eigenstate of the disordered AKLT model.

#### $|2_k\rangle$ state

One can also superpose  $|m, m+n\rangle$  to form the following  $|2_k\rangle$  eigenstate of the AKLT Hamiltonian

$$|2_k\rangle = \sum_{m=0}^{L/2-1} e^{i(k+\pi)m} \sum_n e^{ikn} |n, n+2m+1\rangle, \quad (38)$$

where the lattice momentum  $k$  has to satisfy  $e^{ikL/2} = -1$  for even  $L/2$  and  $e^{ikL/2} = 1$  for odd  $L/2$ . The total number of  $|2_k\rangle$  states is therefore  $L/2$ . Given that  $|n, n+1\rangle$  and  $|n, n+m\rangle$  with  $m \geq 3$  are all annihilated by the disorder term  $\hat{H}_{\text{dis}}$  as discussed previously, all these  $|2_k\rangle$  states remain eigenstates of  $\hat{H}$ . Nevertheless, not all these  $|2_k\rangle$  states are linearly independent with previously discussed scar states, in particular we have the following relation [37]

$$|\mathcal{S}_{L-2}\rangle = \begin{cases} |2_{k=0}\rangle & \text{if } L/2 \text{ is odd;} \\ \sum_{m=0}^{L/2-1} (-1)^m |2_{n=2m+1}\rangle & \text{if } L/2 \text{ is even.} \end{cases} \quad (39)$$

#### $\hat{J}^- |1_\pi\rangle$ state

The previously discussed states,  $|F\rangle$ ,  $|1_k\rangle$ ,  $|2_n\rangle$ , and  $|2_k\rangle$ , are all highest weight states within families of eigenstates of the AKLT Hamiltonian  $\hat{H}_0$ . By acting on these states with the global spin ladder operator  $\hat{J}^- \equiv \sum_n \hat{S}_n^-$ , one generates additional eigenstates of  $\hat{H}_0$  with reduced

total magnetization. Given the relations  $|10\rangle - |01\rangle = \sqrt{2}|J_{1,1}\rangle$  and  $|11\rangle = |J_{2,2}\rangle$ , any neighboring spins of state  $\hat{J}^- |1_\pi\rangle$  only contain components of  $|J_{2,1}\rangle$  and  $|J_{1,0}\rangle$ . Consequently, this state is annihilated by the disorder term,  $\hat{H}_{\text{dis}}$ . Therefore,  $\hat{J}^- |1_\pi\rangle$  remains an eigenstate of the disordered AKLT Hamiltonian  $\hat{H}$ .

#### $\hat{J}^- |1_d\rangle$ state

The previously discussed states account all but one scar state in the disordered AKLT model. To reveal the nature of the missing one, it is easier to start with the following state

$$\begin{aligned} |1_d\rangle &= \sum_n (-1)^n (S_n^-)^2 |F\rangle \\ &= 2 \sum_n (-1)^n | \underbrace{1, \dots, 1}_{n-1}, -1, \underbrace{1, \dots, 1}_{L-n} \rangle. \end{aligned} \quad (40)$$

This state is an eigenstate of  $\hat{H}_0$  as  $|1, -1\rangle - |-1, 1\rangle = \sqrt{2}|J_{1,0}\rangle$  does not contain component of  $|J_{2,m}\rangle$ . However,  $|1_d\rangle$  is linearly dependent with previously discussed scar states, and the missing scar state is actually  $\hat{J}^- |1_d\rangle$ . To demonstrate this, it suffices to show that

$$\langle J_{2,m'} | \hat{J}^- |1_d\rangle = 0, \quad \text{for } m' = -2, -1, 0 \quad (41)$$

which would imply that  $\hat{J}^- |1_d\rangle$  is annihilated by the disorder part  $\hat{H}_{\text{dis}}$ . We can rewrite this relation as follows (for  $m' = -2, -1, 0$ ),

$$\langle J_{2,m'} | J^- |1_d\rangle = \left( \langle 1_d | \hat{J}^+ |J_{2,m'}\rangle \right)^* \delta_{m', -1},$$

where the  $\delta_{m', -1}$  factor arises because the  $j = 2$  components of neighboring spins in  $|1_d\rangle$  only contain  $|J_{2,0}\rangle$  and  $|J_{2,2}\rangle$ . Moreover, the combination  $|1, -1\rangle - |-1, 1\rangle = \sqrt{2}|J_{1,0}\rangle$  does not contain a  $|J_{2,0}\rangle$  component, proving that  $\langle J_{2,m'} | \hat{J}^- |1_d\rangle = 0$  for  $m' = -2, -1, 0$ . Thus,  $\hat{J}^- |1_d\rangle$  is annihilated by the disorder term and is an eigenstate of the disordered AKLT Hamiltonian  $\hat{H}$ . From this, it is also evident why  $(\hat{J}^-)^2 |1_d\rangle$  is not an eigenstate:  $\langle \hat{J}_{2,m'=0}^- | (J^-)^2 \rangle$  has overlap with  $|1, 1\rangle = |J_{2,2}\rangle$  in  $|1_d\rangle$ .

This concludes our discussion of all the numerically identified scar states in the disordered AKLT model. To summarize, the scar states are as follows:

- $L/2 + 1$  SGA scar states  $|\mathcal{S}_{2n}\rangle$ , where we include the ferromagnetic state  $|F\rangle$  in this tower for odd  $L/2$ ;
- $|1_k\rangle$  with a total number  $L$ ;
- $|2_n\rangle$  with  $n = 1, 3, 4, \dots, L/2$  if  $L/2$  is even and  $n = 1, 3, 4, \dots, L/2 - 1$  if  $L/2$  is odd;

- $|2_k\rangle$  with a total number  $L/2$ ;
- Two additional states:  $\hat{J}^- |1_{k=\pi}\rangle$  and  $\hat{J}^- |1_d\rangle$ , where  $|1_d\rangle = \sum_n (-1)^n$ .

Since  $|\mathcal{S}_{L-2}\rangle$  is linearly dependent with  $|2_n\rangle$  and  $|2_k\rangle$ , the total number of scars state is  $5L/2+1$  if  $L/2$  is even, and  $5L/2$  if  $L/2$  is odd. This has been confirmed numerically for  $L = 6, 8, 10$ .

### Appendix B: Scar Eigenoperator Spaces in Disordered AKLT Model

In this section, we provide further details on the eigenoperator spaces of QMBS in the disordered AKLT model (21). As mentioned in the main text, the minimal  $N_0$  of the SGA scars is  $9L + 3$ . Specifically, for tested system sizes ranging from  $L = 6$  to  $L = 16$ , the correlation matrices of the scar states  $|\mathcal{S}_2\rangle, |\mathcal{S}_4\rangle, \dots, |\mathcal{S}_{L-4}\rangle$  have a common null space of dimension  $9L + 3$ . Moreover, this space is a proper subset of the intersection of null spaces of the other SGA scars,  $|\mathcal{S}_0\rangle, |\mathcal{S}_{L-2}\rangle, |\mathcal{S}_L\rangle$ , which is of dimension  $9L + 4$ . This means that there exists an eigenoperator  $\hat{A}$  that can be added to the Hamiltonian to destroy the middle SGA scars  $|\mathcal{S}_2\rangle, |\mathcal{S}_4\rangle, \dots, |\mathcal{S}_{L-4}\rangle$ . This operator  $\hat{A}$  is a sum of local operators

$$\hat{A} = \sum_n (-1)^{n(L-2)/2} \hat{A}_{n,n+1}, \quad (42)$$

and the expression of  $\hat{A}_{n,n+1}$  depends on whether  $L/2$  is even or odd. Omitting the subscript  $(n, n+1)$  for simplicity, we have

$$\hat{A}_{n,n+1} = \lambda_1 \otimes \lambda_2 + \lambda_7 \otimes \lambda_6 - \lambda_2 \otimes \lambda_1 - \lambda_6 \otimes \lambda_7, \quad (43)$$

for odd  $L/2$ , and

$$\begin{aligned} \hat{A}_{n,n+1} = & 3\sqrt{2}(|J_{0,0}\rangle\langle J_{2,0}| + \text{h.c.}) - 7|J_{1,-1}\rangle\langle J_{1,-1}| \\ & + 3|J_{1,0}\rangle\langle J_{1,0}| + 4|J_{1,1}\rangle\langle J_{1,1}| + 11|J_{2,1}\rangle\langle J_{2,1}| \\ & - 11|J_{2,2}\rangle\langle J_{2,2}|. \end{aligned} \quad (44)$$

for even  $L/2$ . Although we have used  $|m_1 m_2\rangle$  and  $|J_{j,m}\rangle$  to make the expression as simple as possible, the final expressions remain cumbersome and difficult to interpret. Conversely, these intricate expressions demonstrate the strength and flexibility of our method. As shown in Fig. 4, the middle SGA scars  $|\mathcal{S}_2\rangle, |\mathcal{S}_4\rangle, \dots, |\mathcal{S}_{L-4}\rangle$  are indeed destroyed when  $c\hat{A}$  ( $c \neq 0$ ) is added to the original Hamiltonian.

The ferromagnetic state  $|F\rangle$ , owing to its simplicity, has the largest eigenoperator space dimension. On the other hand, the ground state of the AKLT Hamiltonian,  $|G\rangle \equiv |\mathcal{S}_0\rangle$ , is unique in that its null space is not a subset of any other scar states, including the ferromagnetic

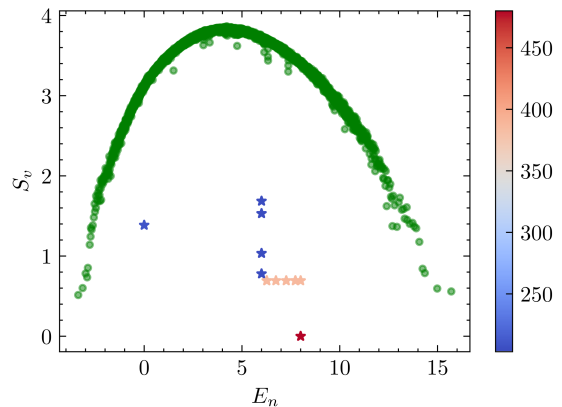


FIG. 4. Plot of bipartite entanglement entropies against the eigenenergies of the Hamiltonian  $\hat{H}' = \hat{H} + c\hat{A}$  for  $L = 8$ , where  $\hat{H}$  is the disordered AKLT Hamiltonian and  $c$  is a real coefficient. As before eigenstates with  $N_0 = 1$  are plotted as green circles, and scar states with  $N_0 > 1$  are drawn as stars, color-coded by their values according to the color bar.

state. This implies that we can construct a Hamiltonian  $\hat{H}'$  of the form

$$\hat{H}' = \hat{H} + \sum_i c_i \hat{A}_i, \quad (45)$$

where  $c_i$  are random real numbers and  $\hat{A}_i$  are eigenoperators  $|G\rangle$  that embeds  $|G\rangle$  as the only scar state. As shown in Fig. 5, such embedding Hamiltonian successfully isolates  $|G\rangle$  as the only scar state.

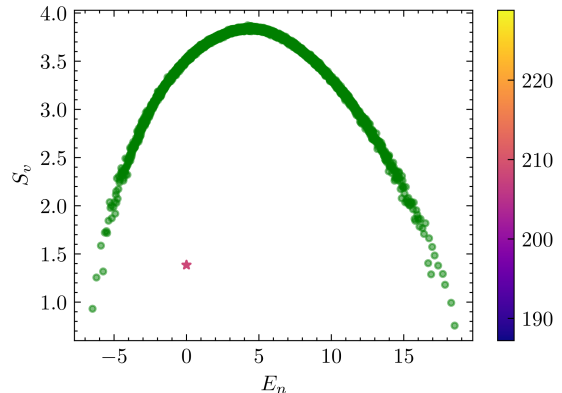


FIG. 5. Plot of eigenenergies against the bipartite entanglement entropies for the embedding Hamiltonian with system size  $L = 8$ . Thermal eigenstates with  $N_0$  are represented as green circles, while scar states with  $N_0 > 1$  are shown as stars, color-coded by their values according to the color bar. We end up with a single scar state, the AKLT ground state  $|G\rangle$ , with  $N_0 = 208$  for the embedding Hamiltonian (45).



### Appendix C: Exact Scars in the Spin-1 XY Model

We next apply our method to the one-dimensional spin-1 XY model whose Hamiltonian is given by

$$\hat{H} = \sum_{\langle ij \rangle} \left( \hat{S}_i^x \hat{S}_j^x + \hat{S}_i^y \hat{S}_j^y \right) + h \sum_i \hat{S}_i^z + D \sum_i (\hat{S}_i^z)^2 + J_3 \sum_i (\hat{S}_i^+ \hat{S}_{i+3}^- + \text{h.c.}), \quad (46)$$

where  $\hat{S}_i^\alpha$  ( $\alpha = x, y, z$ ) are spin-1 operators at site  $i$ ,  $\langle ij \rangle$  denote nearest neighbors,  $h$  is the external magnetic field strength, and  $D$  is the anisotropy parameter. The last term, which couples spins at sites  $i$  and  $i+3$ , is included to break a nonlocal  $SU(2)$  symmetry under open boundary conditions (OBC) [54]. We shall first focus on OBC, where the scar states  $|\mathcal{S}_n\rangle$  admit the following analytic expression,

$$|\mathcal{S}_n\rangle = \mathcal{N}_n (\hat{J}^+)^n |\Downarrow\rangle. \quad (47)$$

Here  $n = 0, 1, \dots, L$ ,  $|\Downarrow\rangle = \otimes_i |m_i = -1\rangle$  is the fully polarized down state,  $\hat{J}^+ = \frac{1}{2} \sum_i (-1)^i (\hat{S}_i^+)^2$  where  $\hat{S}_i^+ = \hat{S}_i^x + i\hat{S}_i^y$  is the ladder operator at site  $i$ . The normalization factor  $\mathcal{N}_n$  is not essential for our discussion. Under OBC, the system exhibits both spatial reflection symmetry and spin inversion symmetry in the zero total magnetization sector, and we shall perform computation in symmetry-resolved sectors. The operator basis  $\hat{L}_i = (\lambda_a \otimes \lambda_b)_{n,n+1}$  is chosen to be the same as that of the spin-1 AKLT model. Since the last term of the Hamiltonian (46) does not belong to the operator space  $\mathcal{V}$ , the Hamiltonian will not manifest itself as a null vector of the correlation matrix. As shown in Fig. 6, all thermal eigenstates have correlation matrix zero  $N_0 = 1$ , which corresponds to the eigenoperator of total magnetization operator  $\hat{M}_z = \sum_i \hat{S}_i^z$ . In contrast, the scar state  $|\mathcal{S}_{L/2}\rangle$  has a significantly larger  $N_0 = 354$ .

For periodic boundary conditions with  $D = 0$ , the model admits another family of scar states [41]

$$|\mathcal{S}'_n\rangle \propto \sum_{i_1 \neq i_2 \neq \dots \neq i_n} (-1)^{i_1 + \dots + i_n} (S_{i_1}^+ S_{i_1+1}^+) \dots (S_{i_n}^+ S_{i_n+1}^+) |\Downarrow\rangle. \quad (48)$$

However, due to a twisted  $SU(2)$  symmetry in even magnetization sectors, we study the following modified Hamiltonian

$$\hat{H} = \sum_{\langle ij \rangle} \left( \hat{S}_i^x \hat{S}_j^x + \hat{S}_i^y \hat{S}_j^y \right) + h \sum_i \hat{S}_i^z + g \sum_i \left[ (\hat{S}_i^+)^2 (\hat{S}_{i+1}^-)^2 + \text{h.c.} \right], \quad (49)$$

where the last term serves to break integrability [44]. This system preserves several symmetries: conservation

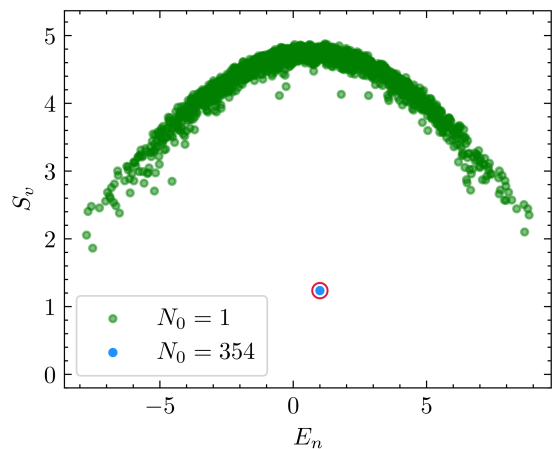


FIG. 6. Plot of bipartite entanglement entropies against the eigenenergies of the spin-1 XY model in the total magnetization  $M_z = 0$  and both spatial reflection and spin inversion antisymmetric sector for system size  $L = 10$ ,  $h = 1.0$ ,  $D = 0.1$ , and  $J_3 = 0.1$ . Eigenstates with the correlation matrix zero  $N_0 = 1$  is marked as green circles. The scar state with  $N_0 = 354$  is circled red.

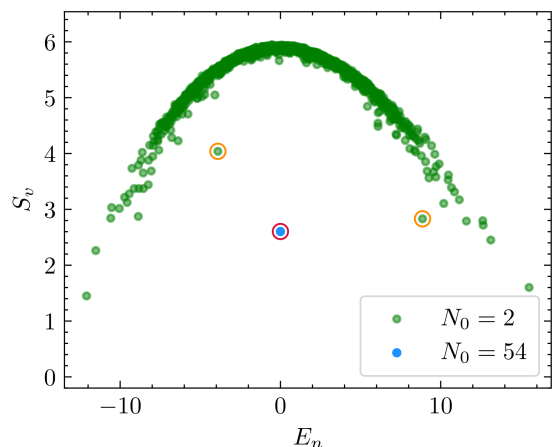


FIG. 7. Plot of bipartite entanglement entropies of eigenstates against the eigenenergies for the spin-1 XY model (49) with system size  $L = 12$ ,  $g = 0.2$ , and  $h = 1.0$ . The symmetry sector corresponds to total magnetization  $M_z = 0$ , lattice momentum  $k = 0$ , and both spatial reflection and spin inversion symmetric.

of total magnetization  $M_z$ , lattice translation, spacial reflection, and spin inversion (which maps  $|m_i\rangle$  to  $| -m_i\rangle$  at site  $i$ ). For our analysis, we focus on the  $M_z = 0$ , lattice momentum  $k = 0$ , and both spatial reflection and spin inversion symmetric sector. The operator basis  $\hat{L}_i = (\lambda_a \otimes \lambda_b)_{n,n+1}$  is chosen to be the same as the disordered AKLT model. As seen in Fig. 7, the thermal eigenstates uniformly have  $N_0 = 2$ , corresponding to the original Hamiltonian and the total magnetization operator  $\hat{M}_z \equiv \sum_i \hat{S}_i^z$ . The scar state  $|\mathcal{S}'_{L/2}\rangle$  is distinguished by having a much larger  $N_0 = 54$ . Although

this scar state can be identified by its low entanglement entropy, the correlation matrix zero  $N_0$  provides a *qualitative* probe rather than a *quantitative* one. Additionally, finite-size effects make it challenging to conclude whether the points circled in orange are scar states or not.

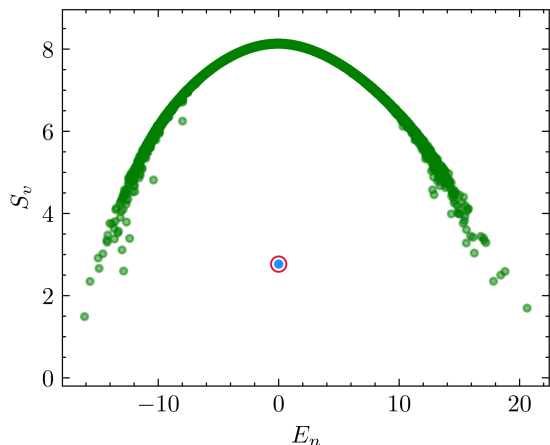


FIG. 8. Plot of bipartite entanglement entropies of eigenstates against eigenenergies for the spin-1 XY model (49) with system size  $L = 16$ . The parameters  $g, h$  and the symmetry sector is the same as that in Fig. 7.

After refining our algorithm, we successfully extended the entanglement entropy spectrum calculation to system size  $L = 16$ . As can be seen from Fig. 8, only the  $E = 0$  state (circled red) has anomalously low entanglement entropy compared to those of surrounding thermal eigenstates, which reinforces our confidence that the points circled in orange in Fig. 7 are not QMBS.

---

\* yaozy@lzu.edu.cn

- [1] R. Nandkishore and D. A. Huse, Many-Body Localization and Thermalization in Quantum Statistical Mechanics, *Annu. Rev. Condens. Matter Phys.* **6**, 15 (2015).
- [2] F. Borgonovi, F. Izrailev, L. Santos, and V. Zelevinsky, Quantum chaos and thermalization in isolated systems of interacting particles, *Phys. Rep.* **626**, 1 (2016).
- [3] L. D'Alessio, Y. Kafri, A. Polkovnikov, and M. Rigol, From quantum chaos and eigenstate thermalization to statistical mechanics and thermodynamics, *Adv. Phys.* **65**, 239 (2016).
- [4] T. Mori, T. N. Ikeda, E. Kaminishi, and M. Ueda, Thermalization and prethermalization in isolated quantum systems: A theoretical overview, *J. Phys. B: At. Mol. Opt. Phys.* **51**, 112001 (2018).
- [5] D. A. Abanin, E. Altman, I. Bloch, and M. Serbyn, Colloquium: Many-body localization, thermalization, and entanglement, *Rev. Mod. Phys.* **91**, 021001 (2019).
- [6] M. Ueda, Quantum equilibration, thermalization and prethermalization in ultracold atoms, *Nat. Rev. Phys.* **2**, 669 (2020).
- [7] J. M. Deutsch, Quantum statistical mechanics in a closed system, *Phys. Rev. A* **43**, 2046 (1991).
- [8] M. Srednicki, Chaos and quantum thermalization, *Phys. Rev. E* **50**, 888 (1994).
- [9] M. Srednicki, The approach to thermal equilibrium in quantized chaotic systems, *J. Phys. A: Math. Gen.* **32**, 1163 (1999).
- [10] V. Dunjko and M. Olshanii, Thermalization from the Perspective of Eigenstate Thermalization Hypothesis, in *Annual Review of Cold Atoms and Molecules*, Annual Review of Cold Atoms and Molecules, Vol. 1 (World Scientific, Singapore, 2012) pp. 443–471.
- [11] J. M. Deutsch, Eigenstate thermalization hypothesis, *Rep. Prog. Phys.* **81**, 082001 (2018).
- [12] F. Franchini, *An Introduction to Integrable Techniques for One-Dimensional Quantum Systems* (Springer, Cham, 2017).
- [13] M. Rigol, V. Dunjko, V. Yurovsky, and M. Olshanii, Relaxation in a Completely Integrable Many-Body Quantum System: An Ab Initio Study of the Dynamics of the Highly Excited States of 1D Lattice Hard-Core Bosons, *Phys. Rev. Lett.* **98**, 050405 (2007).
- [14] L. Vidmar and M. Rigol, Generalized Gibbs ensemble in integrable lattice models, *J. Stat. Mech.* **2016**, 064007 (2016).
- [15] I. V. Gornyi, A. D. Mirlin, and D. G. Polyakov, Interacting Electrons in Disordered Wires: Anderson Localization and Low- $T$  Transport, *Phys. Rev. Lett.* **95**, 206603 (2005).
- [16] D. M. Basko, I. L. Aleiner, and B. L. Altshuler, Metal-insulator transition in a weakly interacting many-electron system with localized single-particle states, *Ann. Phys.* **321**, 1126 (2006).
- [17] M. Rigol, V. Dunjko, and M. Olshanii, Thermalization and its mechanism for generic isolated quantum systems, *Nature* **452**, 854 (2008).
- [18] H. Kim, T. N. Ikeda, and D. A. Huse, Testing whether all eigenstates obey the eigenstate thermalization hypothesis, *Phys. Rev. E* **90**, 052105 (2014).
- [19] H. Bernien, S. Schwartz, A. Keesling, H. Levine, A. Omran, H. Pichler, S. Choi, A. S. Zibrov, M. Endres, M. Greiner, V. Vuletić, and M. D. Lukin, Probing many-body dynamics on a 51-atom quantum simulator, *Nature* **551**, 579 (2017).
- [20] C. J. Turner, A. A. Michailidis, D. A. Abanin, M. Serbyn, and Z. Papić, Weak ergodicity breaking from quantum many-body scars, *Nat. Phys.* **14**, 745 (2018).
- [21] C. J. Turner, A. A. Michailidis, D. A. Abanin, M. Serbyn, and Z. Papić, Quantum scarred eigenstates in a Rydberg atom chain: Entanglement, breakdown of thermalization, and stability to perturbations, *Phys. Rev. B* **98**, 155134 (2018).
- [22] E. J. Heller, Bound-State Eigenfunctions of Classically Chaotic Hamiltonian Systems: Scars of Periodic Orbits, *Phys. Rev. Lett.* **53**, 1515 (1984).
- [23] M. Serbyn, D. A. Abanin, and Z. Papić, Quantum many-body scars and weak breaking of ergodicity, *Nat. Phys.* **17**, 675 (2021).
- [24] S. Moudgalya, B. A. Bernevig, and N. Regnault, Quantum many-body scars and Hilbert space fragmentation: A review of exact results, *Rep. Prog. Phys.* **85**, 086501 (2022).
- [25] A. Chandran, T. Iadecola, V. Khemani, and R. Moessner, Quantum Many-Body Scars: A Quasiparticle Perspective

- tive, *Annu. Rev. Condens. Matter Phys.* **14**, 443 (2023).
- [26] N. Shiraishi and T. Mori, Systematic Construction of Counterexamples to the Eigenstate Thermalization Hypothesis, *Phys. Rev. Lett.* **119**, 030601 (2017).
- [27] K. Pakrouski, P. N. Pallegar, F. K. Popov, and I. R. Klebanov, Many-Body Scars as a Group Invariant Sector of Hilbert Space, *Phys. Rev. Lett.* **125**, 230602 (2020).
- [28] K. Pakrouski, P. N. Pallegar, F. K. Popov, and I. R. Klebanov, Group theoretic approach to many-body scar states in fermionic lattice models, *Phys. Rev. Res.* **3**, 043156 (2021).
- [29] Z. Sun, F. K. Popov, I. R. Klebanov, and K. Pakrouski, Majorana scars as group singlets, *Phys. Rev. Res.* **5**, 043208 (2023).
- [30] J. Ren, C. Liang, and C. Fang, Quasisymmetry Groups and Many-Body Scar Dynamics, *Phys. Rev. Lett.* **126**, 120604 (2021).
- [31] J. Ren, C. Liang, and C. Fang, Deformed symmetry structures and quantum many-body scar subspaces, *Phys. Rev. Research* **4**, 013155 (2022).
- [32] N. O’Dea, F. Burnell, A. Chandran, and V. Khemani, From tunnels to towers: Quantum scars from Lie algebras and  $q$ -deformed Lie algebras, *Phys. Rev. Research* **2**, 043305 (2020).
- [33] C. N. Yang,  $\eta$  pairing and off-diagonal long-range order in a Hubbard model, *Phys. Rev. Lett.* **63**, 2144 (1989).
- [34] C. N. Yang and S. Zhang,  $SO_4$  symmetry in a Hubbard model, *Mod. Phys. Lett. B* **04**, 759 (1990).
- [35] D. K. Mark, C.-J. Lin, and O. I. Motrunich, Unified structure for exact towers of scar states in the Affleck-Kennedy-Lieb-Tasaki and other models, *Phys. Rev. B* **101**, 195131 (2020).
- [36] S. Moudgalya, N. Regnault, and B. A. Bernevig,  $\eta$ -pairing in Hubbard models: From spectrum generating algebras to quantum many-body scars, *Phys. Rev. B* **102**, 085140 (2020).
- [37] S. Moudgalya, S. Rachel, B. A. Bernevig, and N. Regnault, Exact excited states of nonintegrable models, *Phys. Rev. B* **98**, 235155 (2018).
- [38] S. Moudgalya, N. Regnault, and B. A. Bernevig, Entanglement of exact excited states of Affleck-Kennedy-Lieb-Tasaki models: Exact results, many-body scars, and violation of the strong eigenstate thermalization hypothesis, *Phys. Rev. B* **98**, 235156 (2018).
- [39] S. Moudgalya, E. O’Brien, B. A. Bernevig, P. Fendley, and N. Regnault, Large classes of quantum scarred Hamiltonians from matrix product states, *Phys. Rev. B* **102**, 085120 (2020).
- [40] D. K. Mark and O. I. Motrunich,  $\eta$ -pairing states as true scars in an extended Hubbard model, *Phys. Rev. B* **102**, 075132 (2020).
- [41] M. Schechter and T. Iadecola, Weak Ergodicity Breaking and Quantum Many-Body Scars in Spin-1 XY Magnets, *Phys. Rev. Lett.* **123**, 147201 (2019).
- [42] T. Iadecola and M. Schechter, Quantum many-body scar states with emergent kinetic constraints and finite-entanglement revivals, *Phys. Rev. B* **101**, 024306 (2020).
- [43] N. Shibata, N. Yoshioka, and H. Katsura, Onsager’s Scars in Disordered Spin Chains, *Phys. Rev. Lett.* **124**, 180604 (2020).
- [44] S. Chattopadhyay, H. Pichler, M. D. Lukin, and W. W. Ho, Quantum many-body scars from virtual entangled pairs, *Phys. Rev. B* **101**, 174308 (2020).
- [45] Z. Papić, Weak Ergodicity Breaking Through the Lens of Quantum Entanglement, in *Entanglement in Spin Chains: From Theory to Quantum Technology Applications*, edited by A. Bayat, S. Bose, and H. Johannesson (Springer, Cham, 2022) pp. 341–395.
- [46] X.-L. Qi and D. Ranard, Determining a local Hamiltonian from a single eigenstate, *Quantum* **3**, 159 (2019).
- [47] I. Affleck, T. Kennedy, E. H. Lieb, and H. Tasaki, Rigorous results on valence-bond ground states in antiferromagnets, *Phys. Rev. Lett.* **59**, 799 (1987).
- [48] The theoretical analysis is quite involved, and the detailed study is left in Appendix A.
- [49] Refer to Appendix A for details.
- [50] Refer to Appendix B for an in-depth analysis of the scar eigenoperator spaces and scar embedding examples.
- [51] Refer to Appendix C for extra examples of QMBS in the spin-1 XY model which also includes references [54].
- [52] C.-J. Lin and O. I. Motrunich, Exact Quantum Many-Body Scar States in the Rydberg-Blockaded Atom Chain, *Phys. Rev. Lett.* **122**, 173401 (2019).
- [53] S. Moudgalya and O. I. Motrunich, Exhaustive Characterization of Quantum Many-Body Scars using Commutant Algebras (2023), [arXiv:2209.03377](https://arxiv.org/abs/2209.03377) [cond-mat, physics:math-ph, physics:quant-ph].
- [54] A. Kitazawa, K. Hijii, and K. Nomura, An  $SU(2)$  symmetry of the one-dimensional spin-1 XY model, *J. Phys. A: Math. Gen.* **36**, L351 (2003).